



Contents lists available at ScienceDirect

Journal of Orthopaedic Translation

journal homepage: www.journals.elsevier.com/journal-of-orthopaedic-translation

Loss of Bcl-3 delays bone fracture healing through activating NF- κ B signaling in mesenchymal stem cells



Fuxiao Wang^{a,1}, Jiawei Guo^{b,1}, Yili Wang^{a,1}, Yan Hu^a, Hao Zhang^b, Jiao Chen^a, Yingying Jing^a, Liehu Cao^{c,**}, Xiao Chen^{b,***}, Jiacan Su^{a,b,*}

^a Musculoskeletal Organoid Research Center, Institute of Translational Medicine, Shanghai University, Shanghai 200444, China

^b Department of Orthopedics Trauma, Shanghai Changhai Hospital, Naval Medical University, Shanghai 200433, China

^c Department of Orthopedics, Shanghai Baoshan Luodian Hospital, Baoshan District, Shanghai 201908, China

ARTICLE INFO

Keywords:

Bcl-3
Fracture healing
Mesenchymal stem cells
NF- κ B

ABSTRACT

Background: Bone fracture healing is a postnatal regenerative process in which fibrocartilaginous callus formation and bony callus formation are important. Bony callus formation requires osteoblastic differentiation of MSCs.

Materials and methods: The formation of callus was assessed by μ CT, Safranin-O, H&E and Masson trichrome staining. Osteogenesis of MSCs was analyzed by ALP staining, ARS staining, qRT-PCR and WB. And we also used IF and TOP/FOP Flash luciferase reporter to assess the nuclear translocation of PP65.

Results: In this study, we found Bcl-3 showed a significant correlation with bone fracture healing. Results of μ CT showed that loss of Bcl-3 delays bone fracture healing. Safranin-O, H&E and Masson trichrome staining confirmed that loss of Bcl-3 impacted the formation of cartilage and woven bone in callus. Further experiments in vitro manifested that Bcl-3-knockdown could inhibit MSCs osteoblastic differentiation through releasing the inhibition on NF- κ B signaling by Co-IP, IF staining and luciferase reporter assay.

Conclusions: We unveiled that loss of Bcl-3 could lead to inhibited osteogenic differentiation of MSCs via promoting PP65 nuclear translocation.

The translational potential of this article: Our data demonstrated that overexpression of Bcl-3 accelerates bone fracture healing, which serves as a promising therapeutic target for bone fracture treatment.

1. Introduction

Bone fracture is one of the most common traumatic injuries [1,2]. By 2050, the annual number of fractures in China will reach 5.99 million which will cost \$25.43 billion [3]. Fractures seriously affect the quality of human associated with great economic burdens and become a major public health problem.

Fracture healing is a process that could restore damaged skeletal organs to their pre-injury cellular composition, structure, and biomechanical functions. Which involves two stages: anabolic phase to form new skeletal tissues and prolonged catabolic phase to form the original bone

structure [4]. There are many factors affecting fracture healing and bone homeostasis [5]. The therapeutic potential of mesenchymal stem cells (MSCs) for bone healing process has been long proposed and examined.

Caplan coined the term MSCs in 1991 [6]. One of the defining features of MSCs is the tri-lineage differentiation capacity including osteogenesis, chondrogenesis and adipogenesis [7–9]. MSCs were considered to be an appropriate cell source for bone tissue engineering [10]. Promoting MSCs migration and osteogenesis could accelerate fracture healing and the formation of the cambium layer of the periosteum [11–13].

During the osteogenesis of MSCs, the NF- κ B pathway plays a critical

Abbreviations: marrow mesenchymal stem cell, MSCs; B-cell lymphoma 3, Bcl-3; Runt-related transcription factor 2, Runx2; peroxisome proliferator-activated receptor gamma, Ppar- γ ; inhibitor of κ B, I κ B; phosphorylation of P65, PP65; wild type, WT; quantitative reverse transcriptase polymerase chain reaction, qRT-PCR; Micro-computed tomography, μ CT; bone volume per tissue volume, BV/TV; Co-immunoprecipitation, Co-IP; Alkaline Phosphatase, ALP; Alizarin Red S, ARS.

* Corresponding author. Musculoskeletal Organoid Research Center, Institute of Translational Medicine, Shanghai University, Shanghai, 201901, China.

** Corresponding author.

*** Corresponding author.

E-mail addresses: Caoliehu@126.com (L. Cao), sirchenxiao@126.com (X. Chen), drsujacan@163.com (J. Su).

¹ These authors contributed equally to this work

<https://doi.org/10.1016/j.jot.2022.07.009>

Received 9 February 2022; Received in revised form 10 July 2022; Accepted 21 July 2022

role. Several groups have shown that NF-κB signaling could inhibit bone formation through activation of P65 induced by TNFα [14,15]. Overexpression of P65 inhibited BMP-2 and Smad-induced reporter activity to inhibit osteoblast differentiation of MSCs. Overexpression of IκBα could restore the inhibition of overexpressed P65 [16]. In addition to classical IκBs, there are other IκB-like proteins like Bcl-3.

B-cell lymphoma 3 (Bcl-3) is an important member of the IκB family that forms complexes with NF-κB on DNA. The specific biological function of Bcl-3 in MSCs remained poorly understood. Here we explored the roles of Bcl-3 in MSCs during osteogenesis. We discovered that loss of Bcl-3 resulted in the remarkably reduced bony callus volume by influencing the fracture callus and the formation of new bone in vivo. Moreover, Bcl-3-knockdown could suppress the capability of MSCs osteoblasts differentiation through NF-κB P65 signaling.

2. Results

2.1. Loss of Bcl-3 delays bone fracture healing

To assess the effects of Bcl-3 on bone fracture healing, we generated 10-week-old Bcl-3^{-/-} and WT mice. Twenty-one days after surgery, mice were euthanized. X-ray images and radiographic union scores are

considered to be the universal method for grading the stages of bony healing. As shown in Fig. 1A, the number of cortices with bridging callus in Bcl-3^{-/-} group was less than WT group. And the RUST score of WT group was with a mean score of 10 while 6.6 in Bcl-3^{-/-} group (Fig. 1A and B). 3D reconstructions of μCT images of the whole femur, woven bone of callus and cross-section of callus manifested that obvious fracture gaps could be observed in the Bcl-3^{-/-} group and the formation of woven bone of callus was suppressed in Bcl-3^{-/-} group compared with WT group (Fig. 1C). The analysis of μCT suggested that percent of bone volume (BV/TV) and cortical thickness (Ct.Th) was decreased in Bcl-3^{-/-} group and total porosity was increased in Bcl-3^{-/-} group (Fig. 1D and E).

Furthermore, we performed biomechanical testing to detect the mechanical strength of fracture femur detached from WT and Bcl-3^{-/-} mice until day 21 after fracture (Fig. 2A). And our data showed that maximum loading decreased in Bcl-3^{-/-} group compared to WT group (P < 0.05; Fig. 2B). The same result was observed in modulus of elasticity (P < 0.01; Fig. 2C). Therefore, these results revealed that bone mechanical strength was impaired when Bcl-3 was knockout.

2.2. Histological staining of the bone fracture

To further assess the changes in callus, we performed Safranin-O

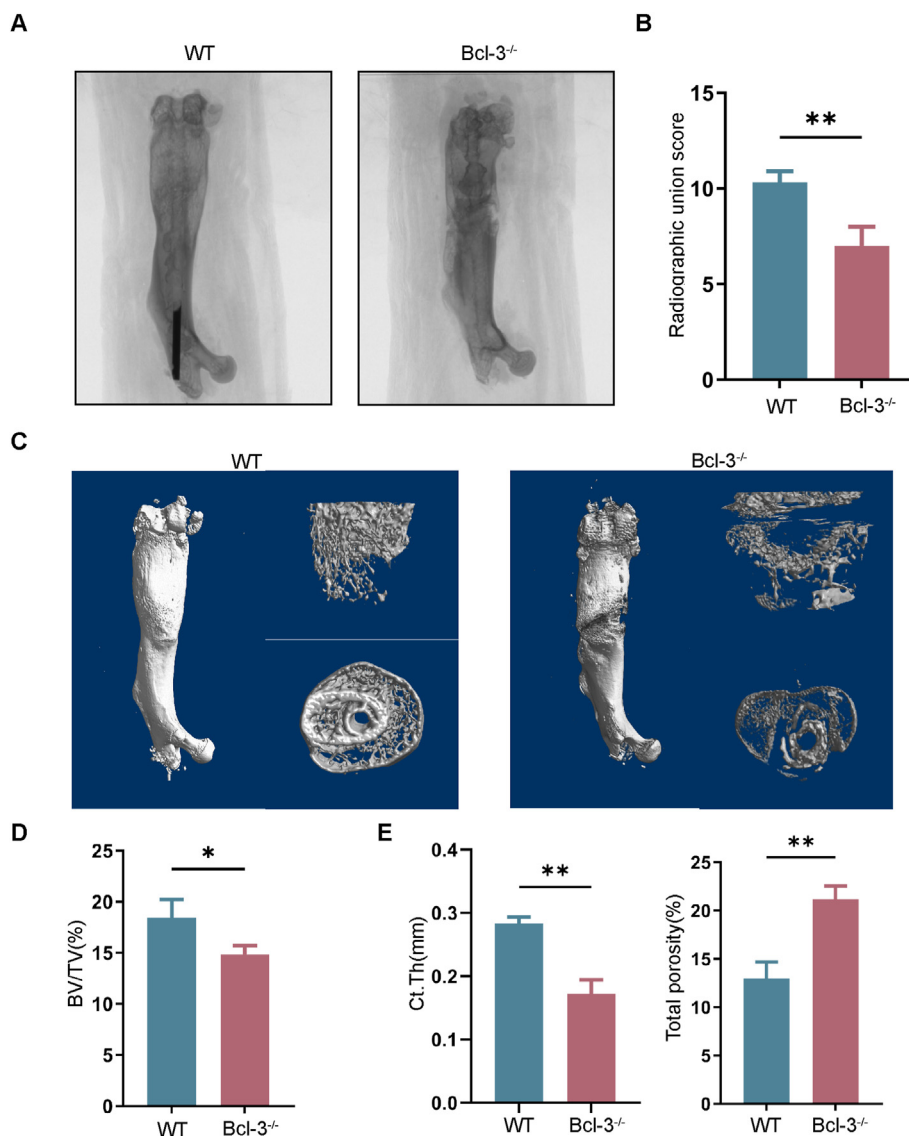


Fig. 1. Loss of Bcl-3 delays bone fracture healing (A–B) X-ray images and radiographic union scores showed clear fracture lines at 21 days after fracture. (N = 3 independent experiments) (C) μCT three-dimensional images of fractured area from 10-week-old male Bcl-3^{-/-} and WT mice at 21 days after fracture. the femoral (left); fractured area of the femoral without cortical bone (right, upper) and the cross section of the fractured area (right, lower) (N = 3 independent experiments) (D) Quantitative measurements of BV/TV of fractured area from 10-week-old Bcl-3^{-/-} and WT mice at 21 days after fracture. (N = 3 independent experiments) (E) Quantitative measurements of Ct.Th and Total porosity of fractured area from 10-week-old Bcl-3^{-/-} and WT mice at 21 days after fracture. (N = 3 independent experiments) The data are presented as the mean ± SD. *P < 0.05; **P < 0.01vs. control group. Statistical analysis was performed using Student's t test.

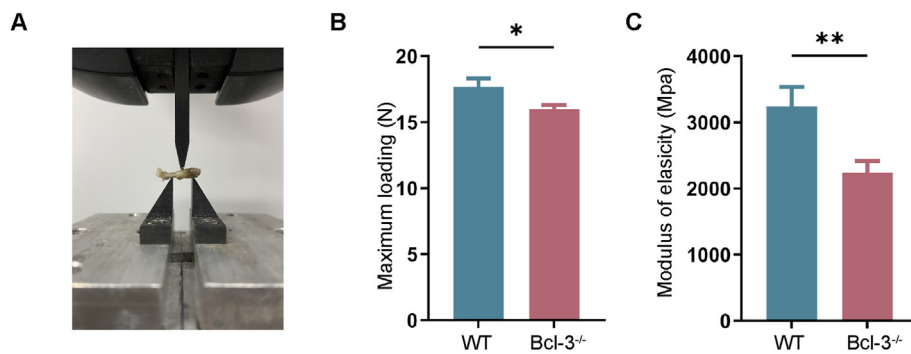


Fig. 2. Biomechanical testing of bone samples from WT and Bcl-3^{-/-} mice, (A) The fractured femur detached from the right leg was used to perform biomechanical testing. (N = 3 independent experiments), (B) Maximum loading was measured in the Bcl-3^{-/-} and control groups. (N = 3 independent experiments), (C) Modulus of elasticity was measured in the Bcl-3^{-/-} and control groups. (N = 3 independent experiments). The data are presented as the mean ± SD. *P < 0.05; **P < 0.01 vs. control group. Statistical analysis was performed using Student's t test.

staining of fracture bone. As shown in Fig. 3A, a significant elevation of cartilage area (CA) and CA/total area (TA) in Bcl-3^{-/-} group compared to WT group. The statistical analysis of CA and CA/TA showed that the percentage of CA/TA was nearly 10% in WT group, versus 20% in Bcl-3^{-/-} group at 14 days after fracture. At 21 days after fracture, the percentage of CA/TA was nearly 5% in WT group, versus 12% in Bcl-3^{-/-} group.

Hematoxylin and Eosin (H&E) and Masson trichrome staining were performed to investigate the new bone formation in the fracture callus. The results of HE revealed that the woven bone formation in callus was decreased in Bcl-3^{-/-} group compared with WT group at 14 and 21 days post-fracture (Fig. 3B). Masson trichrome staining showed that cancellous bone in Bcl-3^{-/-} group was scattered, bone trabeculae was broken and bone collagen was discontinuous compared with WT group at 14 and 21 days post-fracture (Fig. 3C).

2.3. Bcl-3 depletion inhibits MSCs osteoblastic differentiation

Since we have found that the formation of new bone was decreased in Bcl-3^{-/-} group in Fig. 3B, we hypothesized that loss of Bcl-3 inhibits fracture healing by suppressing MSCs osteoblasts differentiation. Therefore, we detected the MSCs osteoblasts differentiation *in vitro*. Firstly, we generated the shBcl-3 lentiviral and the knockdown (KD) efficiency was shown in Fig. 4C detected in MSCs. Alkaline Phosphatase (ALP) and Alizarin Red S (ARS) staining were performed to investigate the capability of MSCs osteoblasts differentiation. After cultured in Mouse Bone Marrow MSCs Complete Culture Medium for 2 days, MSCs were transfected with empty lentiviral shRNA vector or shBcl-3, then cultured in MSCs osteogenic differentiation basal medium for 7 days and 14 days.

The results of ALP and ARS indicated that the area of alkaline phosphatase color development and mineralized nodules calcareous were decreased in 7 days ($p < 0.01$, and $p < 0.001$, respectively) and 14 days ($p < 0.01$, and $p < 0.001$, respectively) when Bcl-3 was KD in MSCs (Fig. 4A and B). The mRNA levels of *Osterix*, *Runx2* and *Ocn* were significantly reduced in shBcl-3 group ($p < 0.001$, $p < 0.05$ and $p < 0.001$, respectively) compared with shCtrl group (Fig. 4C). The same result was improved by protein levels of RUNX2 and OSTERIX (Fig. 4D). Collectively, these data showed that Bcl-3-KD could suppress the capability of MSCs osteoblasts differentiation.

2.4. Bcl-3 interacts with PP65 and regulates nuclear translocation of PP65

NF- κ B signaling is important to maintain bone homeostasis. And P65 was found to inhibit osteoblast differentiation, resulting in the inhibition of bone formation by NF- κ B [16]. To determine whether Bcl-3 regulated bone fracture healing via interacting with PP65, we performed several studies. Firstly, we observed that the protein level of PP65/P65 was increased significantly ($P < 0.001$) when Bcl-3 was knocked down in MSCs (Fig. 5A). Then, we confirmed the interaction between Bcl-3 and PP65 by immunoprecipitation (IP) analysis in MSCs (Fig. 5B). To

examine whether Bcl-3 mediates the transcriptional activity of P65, we transfected TOP/FOP Flash luciferase reporter into Bcl-3-silenced MSCs. The results manifested that the NF- κ B-Luc activity was increased ($P < 0.001$) in Bcl-3 depletion MSCs (Fig. 5C). The results of immunofluorescence showed a rise of nuclear translocation of PP65 when Bcl-3 was knocked down in MSCs (Fig. 5D).

2.5. Overexpression of Bcl-3 accelerates bone fracture healing

Given the function of Bcl-3 in process of bone fracture healing, we generated the Bcl-3 overexpression Adeno-Associated virus (AAV2/9). And the mice were intrafemorally injected with Bcl-3 AAV2/9 or control AAV (5×10^{12} GC/kg) 7 days before the bone fracture surgery. Twenty-one days later, the mice were euthanized. As shown in μ CT of the whole femur, woven bone of callus and cross-section of callus manifested that the fracture gaps were more obvious in WT group and the formation of woven bone of callus was increased in Bcl-3 overexpression group compared with WT group (Fig. 6A). And the RUST score of WT group was with a mean score of 7.6 while 9.6 in Bcl-3 overexpression group (Fig. 6B). Safranin-O staining of fracture bone was performed to assess the changes of callus (Fig. 6C). As shown in Fig. 6C, CA and CA/TA decreased significantly in Bcl-3 overexpressed group at Day 21 compared with WT group, while there is no obvious change in TA (nearly 8% in WT versus 4% in Bcl-3 overexpressed group [CA/TA]).

3. Discussion

In this study, we found that Bcl-3^{-/-} mice had retarded callus formation and inferior mechanical properties. KD of Bcl-3 expression in MSCs resulted in inhibited osteogenic differentiation, downregulated expressions of osteogenesis markers, and increased amount of PP65. Furthermore, the co-IP verified the Bcl-3 bound to PP65, and immunofluorescence staining showed Bcl-3 KD improved the nuclear translocation of PP65. Thus, we revealed that loss of Bcl-3 affected fracture healing and osteoblast generation via promoting NF- κ B P65 signaling.

Fracture healing is a complex process influenced by many factors, such as fracture fixation stability and the blood supply [17,18]. Inflammatory cytokines like TNF- α and the mechanical microenvironment of MSCs are also involved in the process of fracture healing [19–21]. Among them, role of MSCs in fracture healing is non-negligible. Callus mineralization is the hallmark of maturation and fracture union accomplishment, which is related to the generation and function of osteoblasts [22]. Another study showed that *Sostdc1*, which was expressed in the periosteum and crucial to fracture repair, was also expressed in MSCs. The depletion of *Sostdc1* leads to greater callus and more osteoblasts to promote fracture healing [23]. In our research, we found Bcl-3 KD by shRNA *in vitro* could notably suppress their osteogenic differentiation. The ALP and ARS staining and the osteogenic gene expression levels,

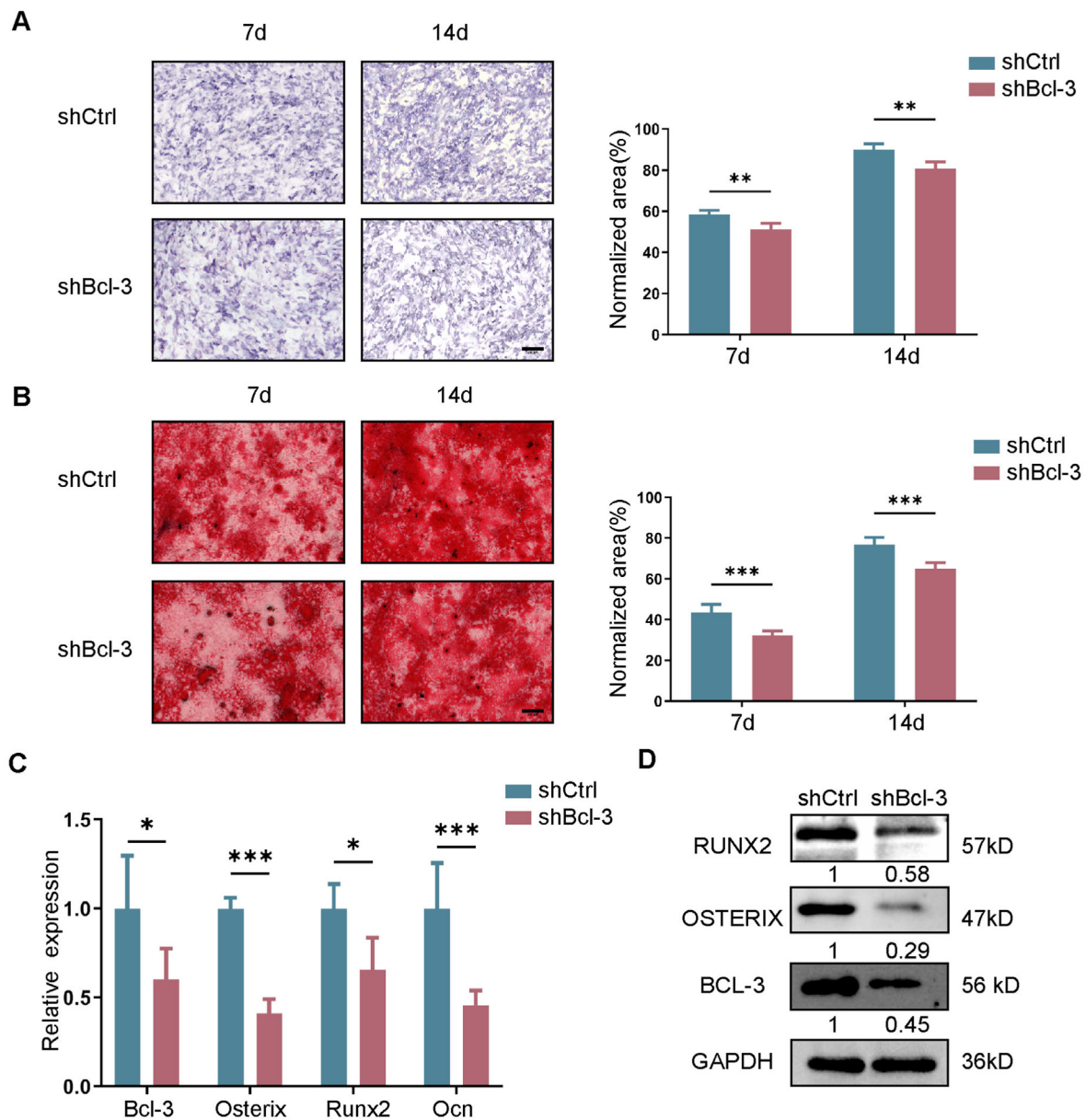


Fig. 4. Bcl-3 depletion inhibits MSCs osteoblastic differentiation (A) Bcl-3 was knockdown in MSCs and cultured in differentiation medium. Cell differentiation was assessed by ALP staining after 7 days and 14 days of osteogenic induction. Scale bar, 200 μ m. (B) Bcl-3 was knockdown in MSCs and cultured in differentiation medium. Cell differentiation was assessed by ARS staining after 7 days and 14 days of osteogenic induction. Scale bar, 200 μ m (C) The expression of Bcl-3, Osterix, Runx2 and Ocn detected by qRT-pcr. (D) The expression of BCL-3, OSTERIX and RUNX2 detected by WB. (N = 3 independent experiments). The data are presented as the mean \pm SD. *P < 0.05; **P < 0.01; ***P < 0.001 vs. control group. Statistical analysis was performed using two-way ANOVA.

including *Osterix*, *Ocn*, and *Runx2* testified that Bcl-3 was prominent to osteoblast generation. Robust osteoblast differentiation substantially promotes fracture repair [24], which is consistent with our findings that Bcl-3 insufficiency contributed to inhibited osteoblast generation and even inferior fracture union.

As we well known, NF- κ B is a major transcription factor regulating inflammatory response and fracture healing [25]. The resolution of inflammation in fracture healing is important, and the inhibition of NF- κ B in skeletal stem cells lead to restore tissue regeneration [26]. In the treatment of bone disease, the development of NF- κ B inhibitors drew most of the attention. For example, as a receptor activator of NF- κ B ligand inhibitor, denosumab is considered to be a specific remedy for prevention of fractures [27]. In NF- κ B signal transduction, the degradation of I κ B is indispensable, which could release the NF- κ B dimer to translocate into the nucleus to regulate the target gene expression [28]. It means that I κ B

has a potential role in the treatment of bone fracture healing. However, as a member of I κ B, the potential effects of Bcl-3 in fracture healing have not been investigated before. In our study, the results of co-IP testified to the hypothesis of the direct bind between Bcl-3 and PP65. And immunofluorescence staining demonstrated that nuclear PP65 was promoted by Bcl-3 KD. Collectively, we identified that Bcl-3 KD upregulated the NF- κ B pathway activity via promoting PP65 nuclear translocation, which might be a reason for Bcl-3 to regulate osteogenic differentiation of MSCs and then affect fracture repair.

During the bone fracture healing, day 14 and 21 are at the stage of endochondral stage and the early remodeling stage, where chondrocytes and osteoblasts play a major role. And fracture healing is completed at 6–8 weeks, where bone remodeling predominates involving both osteoblasts and osteoclasts [4]. In addition, Bcl-3 overexpression significantly decrease TRAP positive osteoclasts and osteoclastic bone resorption in

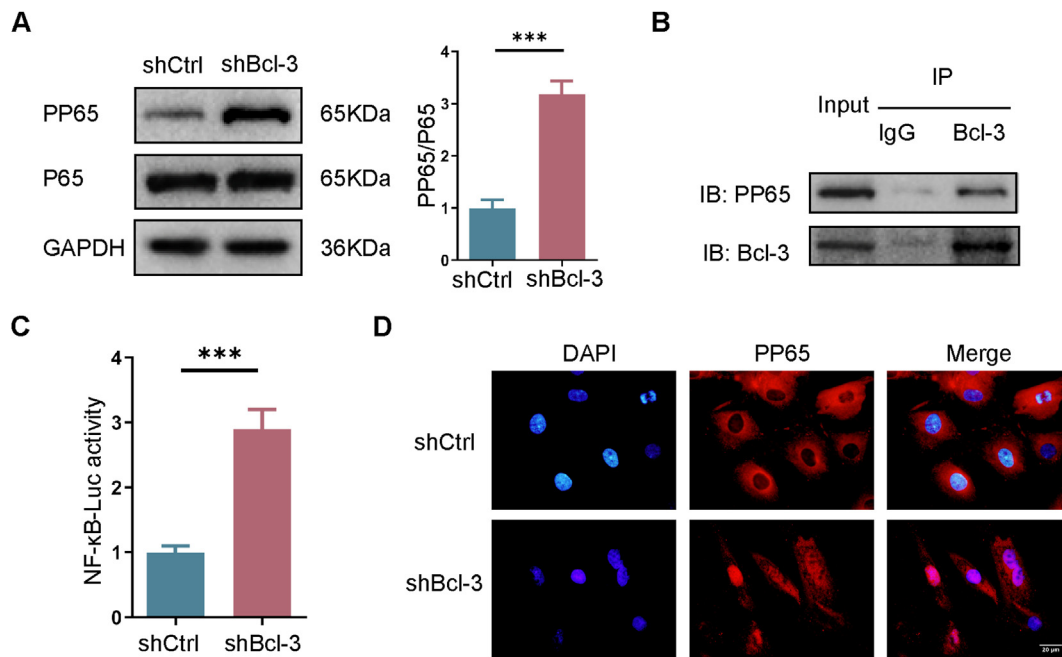


Fig. 5. Bcl-3 interacts with PP65 and regulates nuclear translocation of PP65, (A) Expression of P65 and PP65 in shCtrl and shBcl-3 MSCs detected by WB. (B) Lysates from MSCs were used, and anti-Bcl-3 antibody was used in IP followed by immunoblot using the indicated antibodies (C) MSCs were cotransfected with the shCtrl and shBcl-3 and TOP/FOP Flash reporter plasmid. (D) Immunofluorescence staining of PP65 in shCtrl and shBcl-3MSCs. Scale bar, 20 μ m (N = 3 independent experiments). The data are presented as the mean \pm SD. *P < 0.05; **P < 0.01; ***P < 0.001 vs. control group. Statistical analysis was performed using Student's t test.

the presence of RANKL [29]. In our study, the results showed that Bcl-3 influenced the differentiation of MSCs into osteoblasts, and loss of Bcl-3 inhibited the endochondral bone formation. Based on the above reasons, we did not evaluate the effects of Bcl-3 on the remodeling of hard callus, for Bcl-3 could also affect osteoclastogenesis. Therefore, we did not perform a long-term study at 6–8 weeks. To better illustrate the whole process of bone fracture healing including both mineralization and remodeling, we would better generate the conditional knockout mice. Next, it would be better if we performed detailed mechanisms of Bcl-3 regulating MSCs osteogenic differentiation in this study. For example, we could explore the degradation of PP65 using cycloheximide (CHX) in Bcl-3-silenced MSCs and the expression of PP65 in Bcl-3-overexpressed MSCs. Despite these limitations, we unveiled that loss of Bcl-3 could lead to inhibited osteogenic differentiation of MSCs via increasing PP65 nuclear translocation, thus affecting the callus formation and maturation and causing inferior fracture healing, which remains a potential target in the treatment of bone fracture healing.

4. Experimental model and subject details

4.1. Fracture model

Bcl-3 knockout mice have been described previously (Franzoso et al., 1997) [30] and were obtained from Prof. Xiaoren Zhang [31]. All animals were housed and maintained in pathogen-free conditions. And all animal experiments complied with the ARRIVE guidelines (including study design, sample size, inclusion and exclusion criteria, randomization, blinding, outcome measures, statistical methods, experimental animals, experimental procedures and results) and were carried out in accordance with the National Research Council's Guide for the Care and Use of Laboratory Animals. The protocol was approved by the Ethics Committee of Shanghai University. And the number of mice in each group was three.

Ten-week-old male C57BL/6 and Bcl-3^{-/-} mice were anesthetized with 4% chloral hydrate by intraperitoneal injection. Removed hair from

the skin surface of the right leg and performed a 1.0 cm cut of the skin along the femur after local disinfection. A 26-gauge syringe needle was inserted into the bone marrow cavity through the intercondylar fossa femur. The femur was then transected using a fretsaw to perform an osteotomy. Closed the incision with a 5-0 silk suture [13,32].

4.2. Isolation and culture of primary mouse MSCs

MSCs were isolated from the femur and tibia of 4-week-old C57 mice according to MSCs culture protocol [33] and cultured in OriCell® Mouse Bone Marrow MSCs Complete Culture Medium (cyagen, MUXMX-90011) for 7 days. MSCs preparations with a viability of 85% were used for experiments.

4.3. X-ray and μ CT analyses

2 and 3 weeks after surgery, mice were euthanized. The number of mice in each group was three. Right femurs of mice were collected for X-ray and microcomputed tomography (μ CT) (Skyscan 1275; Bruker μ CT) analyses under the same conditions. Briefly, image acquisition was performed at 50 kV and 60 μ A with a 0.2 rotation between frames. The resolution of the micro-CT images is 11 μ m (pixel size). Semiquantitative analyses of the X-ray were performed according to radiographic union scale (RUST) [34]. CT Analyser (CTAn) and CTvox were used to examine fracture healing quality and form 3D image. During 3 d reconstruction, the number of Layers was 201 and the region of interest is that which remains after the removal of the outermost cortical bone.

4.4. Biomechanical testing

The fracture femurs of the mice were detached from the right leg of bone fracture mice from each group to perform biomechanical testing. The mice were euthanized at 14 and 21 days after surgery. The number of mice in each group was three. Both ends of each femur were placed on the fixator to ensure the fracture site was placed in the middle.

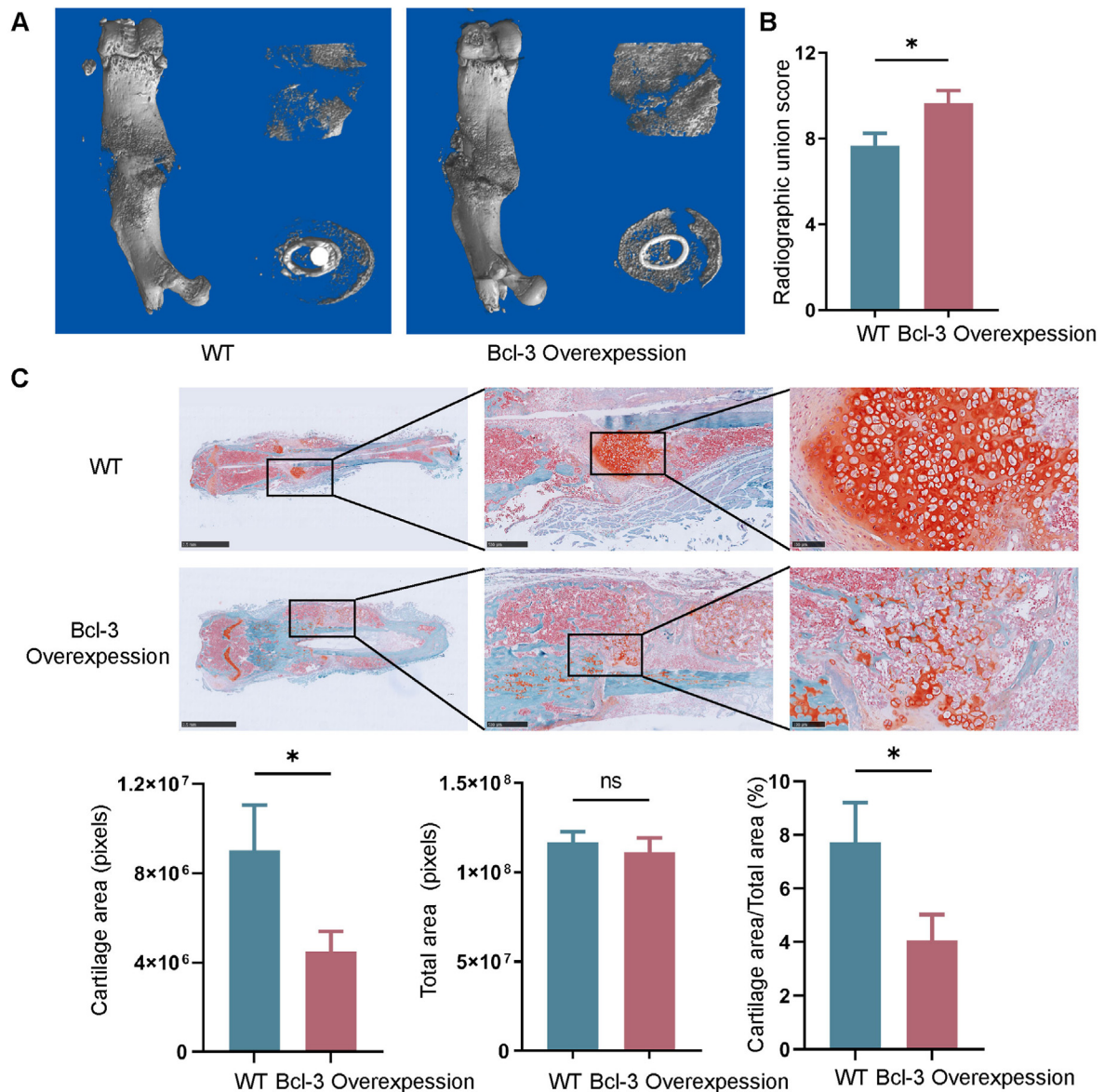


Fig. 6. Overexpression of Bcl-3 accelerates bone fracture healing (A) μ CT three-dimensional images of fractured area from 10-week-old male WT and Bcl-3 overexpressed mice at 21 days after fracture. the femoral (left); fractured area of the femoral without cortical bone (right, upper) and the cross section of the fractured area (right, lower) (B) Radiographic union score of X-ray from 10-week-old male WT and Bcl-3 overexpression mice at 21 days after fracture. (N = 3 independent experiments) (C) Histological sections images and quantitative measurements of the bone fracture with Safranin-O staining. Images show the callus with cortical bone (light blue staining) and cartilage components (indicated in orange). Scale bar, 2.5 mm (left), 500 μ m (middle) and 100 μ m (right). The data are presented as the mean \pm SD. *P < 0.05 vs. control group. Statistical analysis was performed using Student's t test. (For interpretation of the references to color in this figure legend, the reader is referred to the Web version of this article.)

ATS370.7202Bionix was used to apply force at a rate of 1 mm/s until failure to determine the modulus of elasticity and maximum loading of the fracture callus.

4.5. Lentiviral transduction

The empty lentiviral shRNA vector element was pLKD-CMV-EGFP-2A-Puro-U6-shRNA. And the target sequence was CCTGGAGGTTTCGCAAT-TAT. Lentiviral was synthesized by Invitrogen (OBio Technology, Shanghai). Lentivirus supernatant was added to cells and followed by the addition of 1 μ g/ml polybrene.

4.6. qRT-PCR

Total RNA was isolated using TRIzol Reagent (15596-018;

Invitrogen) following protocols of the manufacturer. RNA was reverse transcribed to cDNA by the PrimeScriptTM RT reagent Kit (RR047A, TaKaRa). Quantitative real-time PCR for target genes were performed using SYBR Green (RR420A, TaKaRa). Fold changes were calculated using the equation $RQ = 2^{-\Delta\Delta Ct}$. Each sample was analyzed in triplicate.

4.7. Western blot analysis

Remove the cell culture medium in the petri dish, wash the cells with PBS twice, and remove PBS. Add protein lysate (PMSF; Phosphatase inhibitors; Protease inhibitor; RIPA), and the cells were placed on ice for lysis for 30min. The mixture was centrifuged for at 12,000 \times g for 15min. Protein was quantified using the BCA Protein Assay Kit (P0012S, Beyotime). The protein was separated on 10% sodium dodecyl sulfate-polyacrylamide gel. The Immun-Blot[®] PVDF membrane (1620184, Bio-

Rad) was used in this experiment.

Protein extracts from primary MSCs were analyzed by Western blotting using the antibodies listed as follow: Rabbit monoclonal anti-GAPDH (Abcam, ab181602, 1:10000); Rabbit monoclonal anti-Bcl-3 (Abcam, ab259832, 1:2000); Rabbit monoclonal anti-Osterix (Abcam, ab209484, 1:2000); DyLight® 800 (Abcam, ab201806, 1:20000).

4.8. Immunofluorescence

For immunofluorescence, primary MSCs were seeded in twelve-well plates (6×10^4 cells per well). Cells were plated and grown on coverslips, then washed with PBS and fixed with 4% paraformaldehyde. Cells were blocked with PBS containing 10% FBS and 0.3% Triton-X-100 for 30 min. The proteins were localized using the primary antibodies overnight at 4 °C. The cells were washed and incubated with secondary antibodies. The images were collected with Fluorescence microscope.

4.9. Immunoprecipitation and immunoblotting

Immunoprecipitation and immunoblotting assays were performed as described previously [35]. The following primary antibodies were included: Bcl-3(Abcam, ab209484), P65(Abcam, ab32536), GAPDH (Abcam, ab181602). The secondary antibodies used were as followed: protein A-sepharose (GE17-1279-01, Sigma), Rabbit IgG (sc-2027, Santa Cruz Biotechnology), Mouse IgG (sc-2025, Santa Cruz Biotechnology).

4.10. Luciferase reporter assay

MSCs were cultured in 48-well dishes with a density of 5×10^4 cells/mL and transfected with 250 ng of NF- κ B luciferase reporter plasmid (YEASEN, 11501ES03) and 50 ng of Renilla plasmids as an internal control using Fugene (Roche,04709705001). Cells were collected at 48 hours after transfected with lentivirus and then performed Dual-Luciferase Reporter System (Promega, E1910).

4.11. ALP and ARS staining

For ALP and ARS staining, primary MSCs were seeded in twelve-well plates (6×10^4 cells per well). The medium was replaced with MSCs osteogenic differentiation basal medium (MUBMX-90021, Cyagen) the next day. 2–3 weeks later, cells were with 4% PFA. BCIP/NBT Alkaline Phosphatase Color Development Kit (C3206, Beyotime) and Alizarin Red S Solution (G1450, Solarbio) were used for ALP and ARS staining. Finally, plates were placed in the imaging reader (Cytation 5, BioTek) and photographed for imaging.

4.12. Statistical analysis

Statistical analyses were performed using GraphPad Prism 9.0. Unless otherwise indicated, all experiments were repeated three times and all data were presented as means \pm SD and comparisons between two groups were performed by two-tailed Student's t-test. For more than two groups, we used one-way ANOVA or two-way ANOVA with Tukey's multiple comparisons test. For all statistical tests, $p < 0.05$ was considered statistically significant.

Author contributions

FX.W., JW.G., and YL.W. designed the study, performed the experiments, interpreted the data and wrote the manuscript. J.C., Y.H., H.Z. performed the experiments and interpreted the data. YY.J. designed the study and interpreted the data. J.C. S., X.C., and L.H.C. supervised the project, designed the study. All authors read and approved the final manuscript.

Declaration of competing interest

The author(s) have no conflicts of interest relevant to this article.

Acknowledgements

This work was funded by the National Key Research and Development Plan (2018YFC2001500); National Natural Science Foundation of China (82172098, 81972254, 81871099); Shanghai Rising-Star Program (21QA1412000); Shanghai Municipal Health Commission (202040372).

References

- [1] Mi J, Xu JK, Yao Z, Yao H, Li Y, He X, et al. Implantable electrical stimulation at dorsal root ganglions accelerates osteoporotic fracture healing via calcitonin gene-related peptide. *Adv Sci* 2022;9(1):e2103005.
- [2] Hopkins C, Qin L. Innovative designs and procedures for fracture fixation and soft tissue repair. *J Orthop Translat* 2020;24:A1–2.
- [3] Si L, Winzenberg TM, Jiang Q, Chen M, Palmer AJ. Projection of osteoporosis-related fractures and costs in China: 2010–2050. *Osteoporos Int* 2015;26(7):1929–37.
- [4] Einhorn TA, Gerstenfeld LC. Fracture healing: mechanisms and interventions. *Nat Rev Rheumatol* 2015;11(1):45–54.
- [5] Li X, Wang L, Huang B, Gu Y, Luo Y, Zhi X, et al. Targeting actin-bundling protein L-plastin as an anabolic therapy for bone loss. *Sci Adv* 2020;6(47).
- [6] Caplan AL. Mesenchymal stem cells. *J Orthop Res* 1991;9(5):641–50.
- [7] Chen J, Zhang H, Wu X, Wang F, Wang Y, Gao Q, et al. PTHG2 reduces bone loss in ovariectomized mice by directing bone marrow mesenchymal stem cell fate. *Stem Cell Int* 2021;2021:8546739.
- [8] Hu Y, Li X, Zhang Q, Gu Z, Luo Y, Guo J, et al. Exosome-guided bone targeted delivery of Antagomir-188 as an anabolic therapy for bone loss. *Bioact Mater* 2021;6(9):2905–13.
- [9] Pittenger MF, Mackay AM, Beck SC, Jaiswal RK, Douglas R, Mosca JD, et al. Multilineage potential of adult human mesenchymal stem cells. *Science* 1999;284(5411):143–7.
- [10] Shang F, Yu Y, Liu S, Ming L, Zhang Y, Zhou Z, et al. Advancing application of mesenchymal stem cell-based bone tissue regeneration. *Bioact Mater* 2021;6(3):666–83.
- [11] Zhang Y, Xu J, Ruan YC, Yu MK, O'Laughlin M, Wise H, et al. Implant-derived magnesium induces local neuronal production of CGRP to improve bone-fracture healing in rats. *Nat Med* 2016;22(10):1160–9.
- [12] Sun X, Li X, Qi H, Hou X, Zhao J, Yuan X, et al. MiR-21 nanocapsules promote early bone repair of osteoporotic fractures by stimulating the osteogenic differentiation of bone marrow mesenchymal stem cells. *J Orthop Translat* 2020;24:76–87.
- [13] Zhu J, Liu Y, Chen C, Chen H, Huang J, Luo Y, et al. Cyasterone accelerates fracture healing by promoting MSCs migration and osteogenesis. *J Orthop Translat* 2021;28:28–38.
- [14] Li Y, Li A, Strait K, Zhang H, Nanes MS, Weitzmann MN. Endogenous TNF α lowers maximum peak bone mass and inhibits osteoblastic Smad activation through NF- κ B. *J Bone Miner Res* 2007;22(5):646–55.
- [15] Gilbert L, He X, Farmer P, Rubin J, Drissi H, van Wijnen AJ, et al. Expression of the osteoblast differentiation factor RUNX2 (Cbfa1/AML3/Pebp2 α) is inhibited by tumor necrosis factor- α . *J Biol Chem* 2002;277(4):2695–701.
- [16] Yamazaki M, Fukushima H, Shin M, Katagiri T, Doi T, Takahashi T, et al. Tumor necrosis factor α represses bone morphogenetic protein (BMP) signaling by interfering with the DNA binding of Smads through the activation of NF- κ B. *J Biol Chem* 2009;284(51):35987–95.
- [17] Lin W, Xu L, Zwingenberger S, Gibon E, Goodman SB, Li G. Mesenchymal stem cells homing to improve bone healing. *J Orthop Translat* 2017;9:19–27.
- [18] Cecchi S, Bennet SJ, Arora M. Bone morphogenetic protein-7: review of signalling and efficacy in fracture healing. *J Orthop Translat* 2016;4:28–34.
- [19] Ghimire S, Miramini S, Richardson M, Mendis P, Zhang L. Role of dynamic loading on early stage of bone fracture healing. *Ann Biomed Eng* 2018;46(11):1768–84.
- [20] Zhang L, Richardson M, Mendis P. Role of chemical and mechanical stimuli in mediating bone fracture healing. *Clin Exp Pharmacol Physiol* 2012;39(8):706–10.
- [21] Zhang E, Miramini S, Patel M, Richardson M, Ebeling P, Zhang L. Role of TNF- α in early-stage fracture healing under normal and diabetic conditions. *Comput Methods Progr Biomed* 2022;213:106536.
- [22] Hou Y, Lin W, Li Y, Sun Y, Liu Y, Chen C, et al. De-osteogenic-differentiated mesenchymal stem cells accelerate fracture healing by mir-92b. *J Orthop Translat* 2021;27:25–32.
- [23] Collette NM, Yee CS, Hum NR, Muruges DK, Christiansen BA, Xie L, et al. Sostdcl deficiency accelerates fracture healing by promoting the expansion of periosteal mesenchymal stem cells. *Bone* 2016;88:20–30.
- [24] Mi B, Chen L, Xiong Y, Yang Y, Panayi AC, Xue H, et al. Osteoblast/osteoclast and immune cocktail therapy of an exosome/drug delivery multifunctional hydrogel accelerates fracture repair. *ACS Nano* 2022;16(1):771–82.
- [25] Yongyun C, Jingwei Z, Zhiqing L, Wenxiang C, Huiwu L. Andrographolide stimulates osteoblastogenesis and bone formation by inhibiting nuclear factor kappa-Beta signaling both in vivo and in vitro. *J Orthop Translat* 2019;19:47–57.

- [26] Ko KI, Syverson AL, Kralik RM, Choi J, DerGarabedian BP, Chen C, et al. Diabetes-induced NF-kappaB dysregulation in skeletal stem cells prevents resolution of inflammation. *Diabetes* 2019;68(11):2095–106.
- [27] Pang KL, Low NY, Chin KY. A review on the role of denosumab in fracture prevention. *Drug Des Dev Ther* 2020;14:4029–51.
- [28] Lin TH, Pajarinen J, Lu L, Nabeshima A, Cordova LA, Yao Z, et al. NF-kappaB as a therapeutic target in inflammatory-associated bone diseases. *Adv Protein Chem Struct Biol* 2017;107:117–54.
- [29] Wang K, Li S, Gao Y, Feng X, Liu W, Luo R, et al. BCL3 regulates RANKL-induced osteoclastogenesis by interacting with TRAF6 in bone marrow-derived macrophages. *Bone* 2018;114:257–67.
- [30] Franzoso G, Carlson L, Scharon-Kersten T, Shores EW, Epstein S, Grinberg A, et al. Critical roles for the Bcl-3 oncoprotein in T cell-mediated immunity, splenic microarchitecture, and germinal center reactions. *Immunity* 1997;6(4):479–90.
- [31] Zhang X, Paun A, Claudio E, Wang H, Siebenlist U. The tumor promoter and NF-kappaB modulator Bcl-3 regulates splenic B cell development. *J Immunol* 2013;191(12):5984–92.
- [32] Martineau C, Kaufmann M, Arabian A, Jones G, St-Arnaud R. Preclinical safety and efficacy of 24R,25-dihydroxyvitamin D3 or lactosylceramide treatment to enhance fracture repair. *J Orthop Translat* 2020;23:77–88.
- [33] Huang S, Xu L, Sun Y, Wu T, Wang K, Li G. An improved protocol for isolation and culture of mesenchymal stem cells from mouse bone marrow. *J Orthop Translat* 2015;3(1):26–33.
- [34] Whelan DB, Bhandari M, Stephen D, Kreder H, McKee MD, Zdero R, et al. Development of the radiographic union score for tibial fractures for the assessment of tibial fracture healing after intramedullary fixation. *J Trauma* 2010;68(3):629–32.
- [35] Chen X, Cao X, Sun X, Lei R, Chen P, Zhao Y, et al. Bcl-3 regulates TGFbeta signaling by stabilizing Smad3 during breast cancer pulmonary metastasis. *Cell Death Dis* 2016;7(12):e2508.